Regular article

Chen Chen, Xun Hou and Jinhai Si*

Design of an integrated optics for transglutaminase conformational change

https://doi.org/10.1515/ntrev-2018-0022
Received March 1, 2018; accepted May 7, 2018

Abstract: A detailed theoretical research on a novel integrated optics with surface plasmon resonance (SPR)-based waveguide is presented. An SPR multilayer section is designed by introducing intermediate layers to support fundamental mode and stronger electromagnetic field. Most current techniques excited with a single optical mode are "blind" to the conformational change of bound molecules. The greatest strength of such technique lies in monitoring protein conformational change. The Mach-Zehnder interferometry architecture is adopted to maximize sensor sensitivity and prevent unspecific binding from biological material and error from geometrical difference. A proof-of-concept is conducted on the integrated optics by detecting protein transglutaminase (tTG) specifically binding calcium ion (Ca^{2+}) via the finite-element method. The minimum decrease of biolayer thickness ($\delta_a = 0.5$ nm) caused by tTG-Ca^{2+} interaction is much smaller than a single protein molecule (normally 1–100 nm). Associated with biolayer thickness and density, a thin dense layer is formed as Ca^{2+} binds to the tTG protein. Thus, the tTG protein undergoing conformational change on binding Ca^{2+} is traced and verified as molecular interaction occurs.

Keywords: dual polarizations; finite-element method; integrated optics; protein conformational change.

***Corresponding author: Jinhai Si,** Key Laboratory for Physical Electronics and Devices of the Ministry of Education and Shaanxi Key Lab of Information Photonic Technique, School of Electronics and Information Engineering, Xi'an Jiaotong University, Xi'an 710049, China, e-mail: jinhaisi@mail.xjtu.edu.cn
Chen Chen and Xun Hou: Key Laboratory for Physical Electronics and Devices of the Ministry of Education and Shaanxi Key Lab of Information Photonic Technique, School of Electronics and Information Engineering, Xi'an Jiaotong University, Xi'an 710049, China

1 Introduction

Label-free optical biosensors present good performance in detecting biological systems with high sensitivity and multiparameter analysis, thereby promoting significant advances in clinical diagnostics, drug discovery, food process control, and environmental monitoring [1]. In addition, they could be implemented in lab-on-a-chip that can test at the point-of-care (POC) with lower cost [2]. Specifically, the measurement is easier to carry out and allows for quantitative and kinetic detection of molecular interaction. The detection principle of most optical biosensors is based on the evanescent field [3]. Currently, the bioreceptor layer is immobilized onto the sensor surface. The exposure to the partner analytes promotes molecular recognition and thus slightly alters the biolayer thickness (a) and refractive index (n_l). As a result, the effective mode index sensed by the evanescent tail is affected via such modification. As the evanescent wave decays exponentially into the bulk solution with a decay length on the order of 0.1–1 μm [3], it only detects changes taking place on the surface of the chip. Thus, nonspecific reactions can be removed as any changes in the bulk solution will hardly influence the sensor response. Such advantage makes the evanescent-based biosensors the most promising techniques for the detection of targets in complex real samples.

Among various evanescent wave biosensors, integrated Mach-Zehnder interferometers (MZI) are not only easier in design, fabrication, and measurement but also offer the prospect of making a portable POC device for biosensing. Integrated MZI has particular significance due to its intelligent association with very sensitive methods, waveguiding and interferometry, bringing about a new generation of biosensors. Using the merits of these two approaches, the integrated MZI still maintains mechanical stability, capability in mass production, and miniaturization [4]. Such device has a broad dynamic range and long interaction length. Moreover, it has been demonstrated that the inherent reference arm is capable of reducing common mode noises [5], including temperature fluctuation and nonspecific adsorption.

Surface plasmon (SP) resonance (SPR)-based sensors are continuously attractive to the researchers for its outstanding performance in monitoring complex molecular interactions [6]. Particularly, optical waveguide-based SPR has an extra advantage over traditional SPR devices for their possible integration with other optical components on a single chip [7]. The principle of these sensors is the coupling of electromagnetic energy between a guided mode and a SP mode. An SP wave (SPW) is excited by the incident light whose wave vector matches that of SPW. The position of the SPR dip in the spectrum relies on the refractive index of the sensed medium as the propagation constant of SP is extremely sensitive to the shifts in refractive index distribution within the evanescent field. To maximize the sensitivity of such device, the selection of the metal and introduction of the intermediate layer are widely investigated. For example, Nenninger et al. [8] have reported that the sensitivity can be achieved seven times more than that of conventional SPR when introducing an intermediate layer of Teflon.

However, due to the single measurement of transverse magnetic (TM) polarization, SPR-based sensor is unable to differentiate between shifts in the biolayer thickness Δa and refractive index of layer Δn_l without ambiguity. That means such technology is "blind" to the conformational change of bound molecules. To characterize the conformational change of biomolecules, two measurements via dual polarization are required. Optical waveguide lightmode spectroscopy potentially using more than two modes is employed in measuring the adsorbed protein [9]. The approach is expensive and bulk and thereby not compatible with the concept of POC. Dual polarization interferometry [10], with its ability to monitor conformational change in molecules, has been deployed in the field of protein engineering. This commercially available technique lacks multiplexing abilities and suffers from a large footprint, setting limits on the development and application as a biosensor [3].

In this article, we initially design an SPR-based optical waveguide with an SPR multilayer section consisting of a Si core and two Ag strips between which two open nanoslots are formed. Nanoslots that are exposed to the test analyte can support a mixture between guided mode and SP mode with relatively low propagation loss. Both transverse electronic (TE) and TM modes are strongly confined to the slots. Afterward, the proposed SPR-based waveguide is incorporated onto MZI to maximize sensitivity and prevent unspecific binding from biological material and error from geometrical difference. The conformational change of the protein transglutaminase (tTG) is further characterized by the device. tTGs are enzymes that are involved in the posttranslational modification of proteins and are widespread in both extracellular and cellular fluids. The activities of protein modification by tTG play a vital role in programmed cell death, cytoskeletal proteins, and cross-linking membrane [11]. It has been shown that such activities are modulated by calcium ions (Ca^{2+}) and guanosine triphosphate (GTP). The modulation is correlated with the conformational change induced by modulators (Ca^{2+} and GTP). The whole process of tTG-Ca^{2+} ion interaction is simulated based on the finite-element method (FEM) with success. Power change detection is employed to interpret the refractive index change in that constant position of resonance dips with significant intensity amplitude presented in the output spectrum. Such detection is more sensitive to a small change of refractive index [12] and can be fulfilled via an optic-electric detector with minimum cost.

2 Design of an SPR-based biosensor

2.1 Architecture of SPR-based waveguide

SPR-based waveguide is the heart of the integrated optics. We consider an SPR-based optical waveguide consisting of two identical Ag strips and an SPR multilayer section located on the SiO_2 substrate. The Si core of the SPR section is coated with two metal layers (Cr and Ag layers), above which lies an intermediate layer Ta_2O_5. As a result, the fundamental TM polarized SP mode can be supported effectively on the surface of the multilayer. Two identical Ag strips are placed on opposite sides of the SPR section with a distance of nanometers; thus, the TE mode is confined to the lateral nanoslots. In the simulation, thicknesses of silica substrate, Si region, metallic layers, and the intermediate layer are taken as $h_{SiO2} = 3$ μm, $h_{Si} = 550$ nm, $h_{Cr} = h_{Ag} = h_{Ta2O5} = 5$ nm. The width of the Si core and the thickness of the Ag strip are set as $w_{Si} = 750$ nm and $h_{Ag} = 565$ nm. The lateral nanoslot formed between the Si rib and Ag strip is taken as $w_{slot} = 50$ nm. The wavelength-dependent refractive indices of Si [13] and SiO_2 [14] regions are achieved by a previous literature. The Cr layer is modeled using experimental data from Johnson and Christy [15] and that of the Ta_2O_5 intermediate is gained using literature data [16]. The Drude-Sommerfeld mode is adopted to characterize the dielectric function of Ag [17]. The operation wavelength spans $1.280\ \mu m \le \lambda \le 1.315\ \mu m$. (central wavelength 1.3 μm). The wavelength selection [18] is based on a tradeoff between the absorption loss caused by aqueous solution

and the broadband light sources. Water solution optical absorption is smaller at wavelength of 1.3 μm compared to the 1.55 μm wavelength commonly used for operation. The cross-section view of the proposed structure is shown in Figure 1A. For such a configuration, the SPR-based waveguide is found to strongly support both TE and TM polarized modes, which are presented in the field profile (Figure 1B) obtained via simulation based on FEM.

2.2 Theory of SPR-based waveguide

For the SPR multilayer section, incident light is fed to the Si core and excited a TM polarized SPW on the surface of the multilayer when the phase velocities of the optical mode matches that of the SPW. Because the refractive index of Ag (the real part) is significantly different from the index of dielectric waveguide (Si core), layer Cr is introduced to greatly promote the phase match between the guided mode and SP mode. As a result, the electromagnetic field is enhanced at the surface of the multilayer and the sensitivity is improved as well. Meanwhile, a TE polarized SPW is excited in the lateral nanoslots between the Ag strip and Si rib. Two measurements simultaneously provided by dual polarization optogeometrical properties (density and thickness) of the protein layers can be determined without ambiguity. As a result, a dip in the output spectrum is observed at specific wavelength for dual polarization and the coupling of electromagnetic energy between a guided mode and an SP mode occurs. The amplitude of resonance dip strongly relies on the refractive index of the sensed medium. Any changes of the sensed medium will alter the resonance condition, which results in a shift of the resonance dip. Evidently, nanoslots are able to store electromagnetic energy resulting in subwavelength optical guiding with lower propagation loss. The dielectric discontinuity at the Si core-solution interface produces a polarization charge [19] that interacts with the plasma oscillations of the metal-solution interface. The gap region can be equated with an effective optical capacitance [19] resulting in strong field confinement and longer propagation distance. We take intensity to evaluate refractive index changes. Power change detection is more sensitive to a small change in the refractive index of the ambient medium [12]. Such detection can be achieved simply using an optic-electric detector, thus significantly cutting the experiment cost. With the introduction of MZI, not only the common mode noise and drift in the detection can be reduced greatly but also the control trial can be done.

2.3 Modal investigation

In this section, we will discuss the influence of the intermediate layer on the sensitivity of SPR-based waveguide. Cr film is capable of promoting the conversion of the guided mode in the Si rib to the SP mode on the outer surface of the multilayer and supporting the fundamental SP mode. The field profile is shown in Figure 2. The profile of the electromagnetic field, especially for the TM mode, is smooth and continuous, thereby supporting the fundamental mode on the Cr layer surface. However, the one without Cr film supporting multimode might lead to spurious measurement. The sensitivities of the biosensor are improved by introducing a Ta_2O_5 intermediate layer for dual polarizations and the results are shown in Figure 3. The amplitude of intensity is increased with regard to the structure with Ta_2O_5 film; thus, the sensitivity is expected to be enhanced. The increased values of intensity (dP) are 0.02 and 0.05 for dual polarization. Moreover, we consider the influence of multilayer thickness on the effective mode index n_{eff} and propagation loss of SPR-based

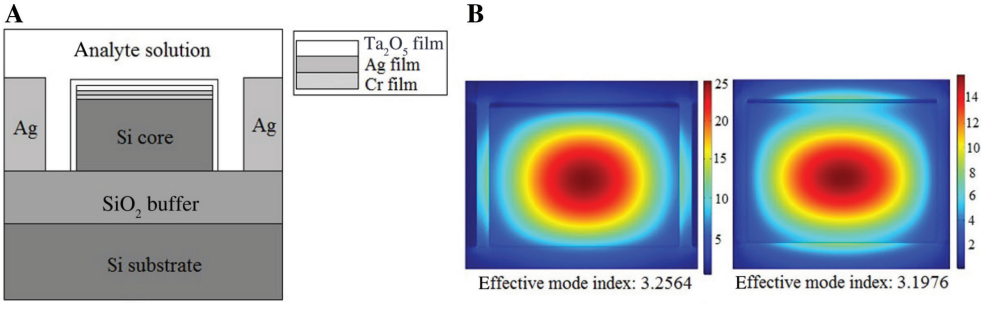

Figure 1: The SPR-based waveguide consisting of two identical silver strips and between which an SPR multilayer section is located. Highly confined hybrid modes with dual polarizations are supported in this structure. Thus, the refractive index of biolayer and its thickness can be measured individually and without ambiguity. The greatest strength of such technique lies in monitoring protein conformational change. (A) Cross-section view of SPR-based waveguide and (B) field profile of SPR-based waveguide for dual polarization.

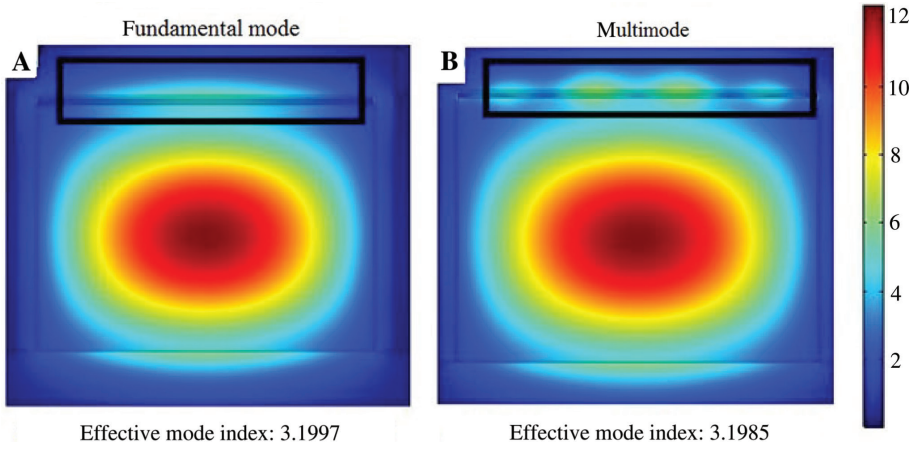

Figure 2: Field profile of SPR-based waveguide with respect to TM mode: (A) with Cr layer and (B) without Cr layer.

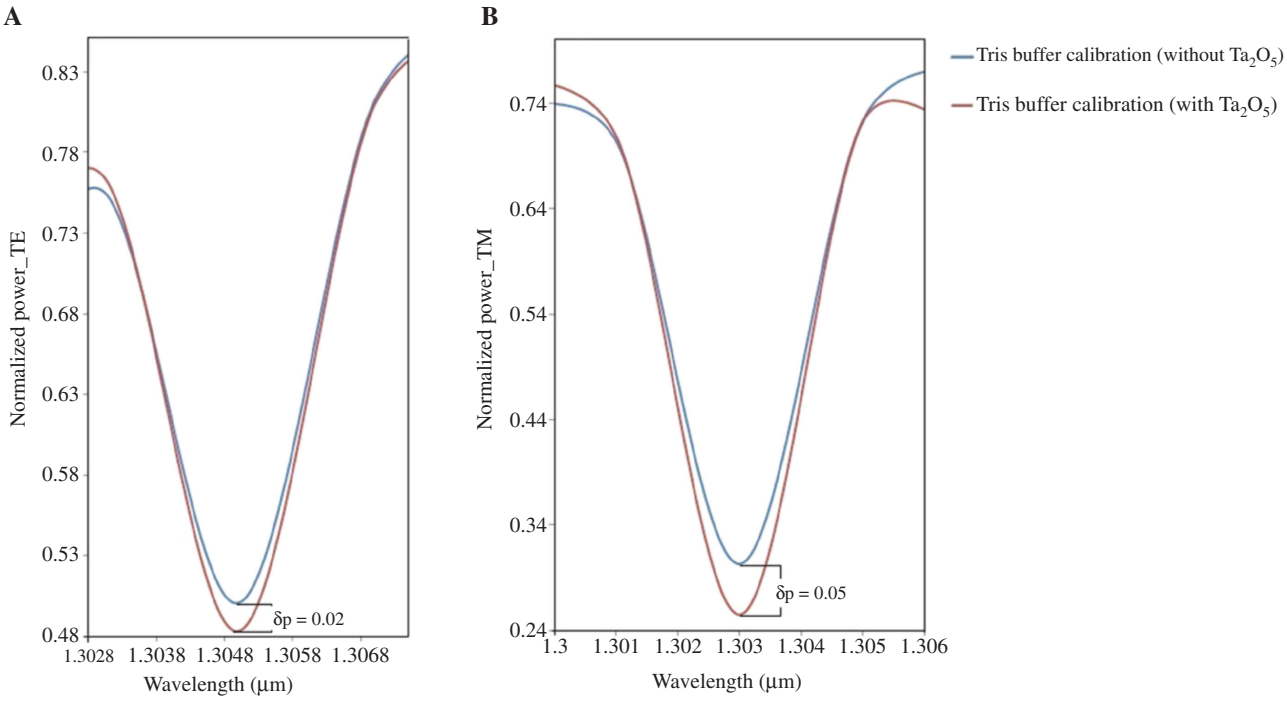

Figure 3: Output spectrum of Tris buffer calibration for SPR-based waveguide with or without Ta_2O_5 layer: (A) TE mode and (B) TM mode.

waveguide for both TE and TM modes. The thickness of the metallic layer plays a key role in the excitement of SPW [20]. If the metal is too thin, the SPW will be greatly damped due to radiation damping into the Si rib. The thicker metallic film might prevent the excitation of SPW because of the adsorption in the metal. To simplify the research, thickness per layer is set as an equal value. The data are plotted in Figure 4. Effective mode indices increase with thinner multilayer. The propagation losses achieve the minimum decay value when the multilayer thickness decreases. Thus, the optimum structure of the proposed SPR waveguide with thickness of 5 nm per film (Ag, Cr, and Ta_2O_5) is adopted and subsequently implemented on the arms of MZI.

3 Characterization of integrated optics

3.1 Architecture of integrated optics

The optimized SPR-based waveguide is incorporated onto the arms of MZI afterward and the model is sketched in

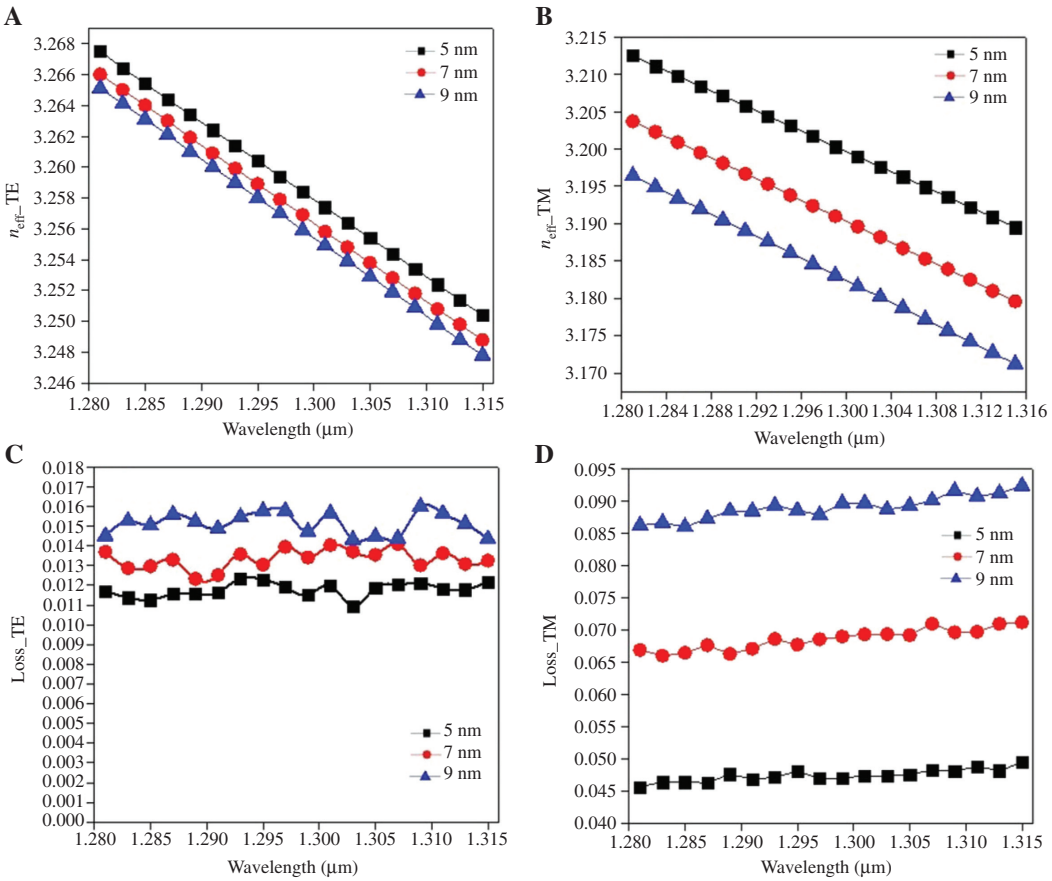

Figure 4: The effective mode index n_{eff} dependent on the thickness of multilayer. (A) for TE mode and (B) for TM mode. The propagation loss dependent on the thickness of multilayer. (C) for TE mode and (D) for TM mode.

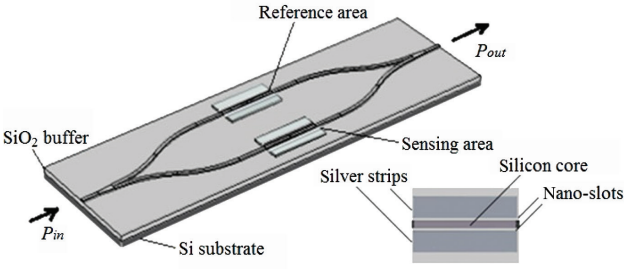

Figure 5: 3D schematic structure of integrated MZI with SPR-based waveguide. Inset figure amplifies the interaction area.

Figure 5. The lengh of the device is 80 μm (L = 80 μm). The sensing and reference arms with identical length L_m = 20 μm are separated by the distance D = 15 μm. The Y-splitter is composed of S-shaped bent wires with a bending radius of 23 μm (r_0 = 23 μm). The length (l) and width (w) of SPR-based waveguide are 1 and 7 μm, respectively. Cytop (http://www.bellexinternational.com/products/cytop/) cladding, which aims to avoid external interference, is employed to cover the designed structure with window opened for injecting solution.

3.2 Protein analysis based on integrated optics

Generally, the tTG-Ca^{2+} binding event can be simplified to four distinct steps: (1) Tris buffer flowing over the waveguide surface for initial calibration; (2) BS_3, an amine-amine linker immobilized on the waveguide surface; (3) capture of protein tTG onto the surface via the BS_3 layer; and (4) introduction of Ca^{2+} to bind with protein tTG. To prevent unspecific interaction and external effects, the control surface is designed without adding protein solution. During the biological event, the thickness a and refractive index n_l of the protein layer with known numerical value were obtained from typical literature data [21] and collected in Table 1. Comparing the covering solution exposed to the two arms, one can find that Tris buffer instead of tTG protein is flowed over the reference arm in

Table 1: Layer characteristics of biolayer properties (refractive index and thickness) and bulk solution during the process of molecular interaction [21].

Material	Bulk index	Biolayer index	Biolayer thickness (nm)
Working surface with protein			
Tris buffer	1.3337	0	0
BS_3	1.3337	1.4533	1.698
tTG	1.3337	1.4184	5.261
Ca^{2+}	1.3337	1.4284	4.761
Control surface without protein			
Tris buffer	1.3337	0	0
BS_3	1.3337	1.4533	1.698
Tris buffer	1.3337	1.4533	1.698
Ca^{2+}	1.3337	1.4533	1.698

step 3. In this way, the parallel control trial is realized to prevent unspecific binding from biological material and error from geometrical difference. In the biological event, bulk solution remains constant with a refractive index of 1.3337. Resonance phenomena appear but without marked intensity difference in the output spectrum with respect to the pure SPR-based waveguide. The reason probably comes from that the bulk refractive index remains unchanged and the bulk solution has dominant influence on the effective mode index of the waveguide. Moreover, the difference of optogeometrical properties (refractive index and thickness) between the tTG layer and layer tTG bound with Ca^{2+} is too tiny ($\delta_a = 0.5$ nm) to be identified by the pure waveguide. To maximize the sensitivity, we incorporated the proposed waveguide onto MZI. As expected, resonance dips with different intensity at specific wavelength are presented in the output spectrum. The magnitude of the resonance dip in the received power is dependent on the conversion of SPW. The MZI improves the efficiency of the mode conversion and thus functions as an amplifier with regard to the sensitivity. The results are shown in Figure 6. It is obvious that resonance dips with different amplitude representing each step in the molecular interaction.

3.3 Characterization of protein conformation

To extract biolayer thickness and refractive index, we investigated the relation between power variations and properties of the protein layer (refractive index and thickness) at resonance dips for dual polarizations and defined the expression as follows:

$$\begin{bmatrix} \Delta P_{TE} \\ \Delta P_{TM} \end{bmatrix} = \begin{bmatrix} \frac{\partial P_{TE}}{\partial n_l} & \frac{\partial P_{TE}}{\partial a} \\ \frac{\partial P_{TM}}{\partial n_l} & \frac{\partial P_{TM}}{\partial a} \end{bmatrix} \cdot \begin{bmatrix} \Delta n_l \\ \Delta a \end{bmatrix} \tag{1}$$

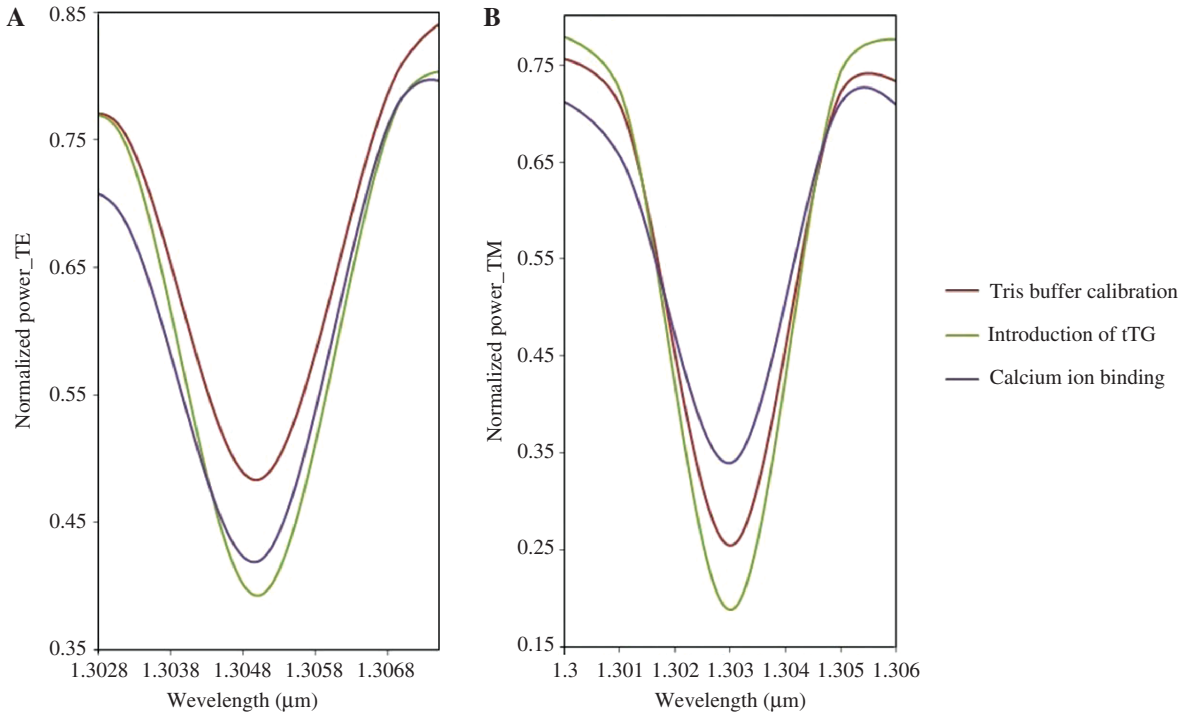

Figure 6: Output spectrum of protein tTG interaction with Ca^{2+} for the integrated MZI biosensor: (A) TE mode and (B) TM mode.

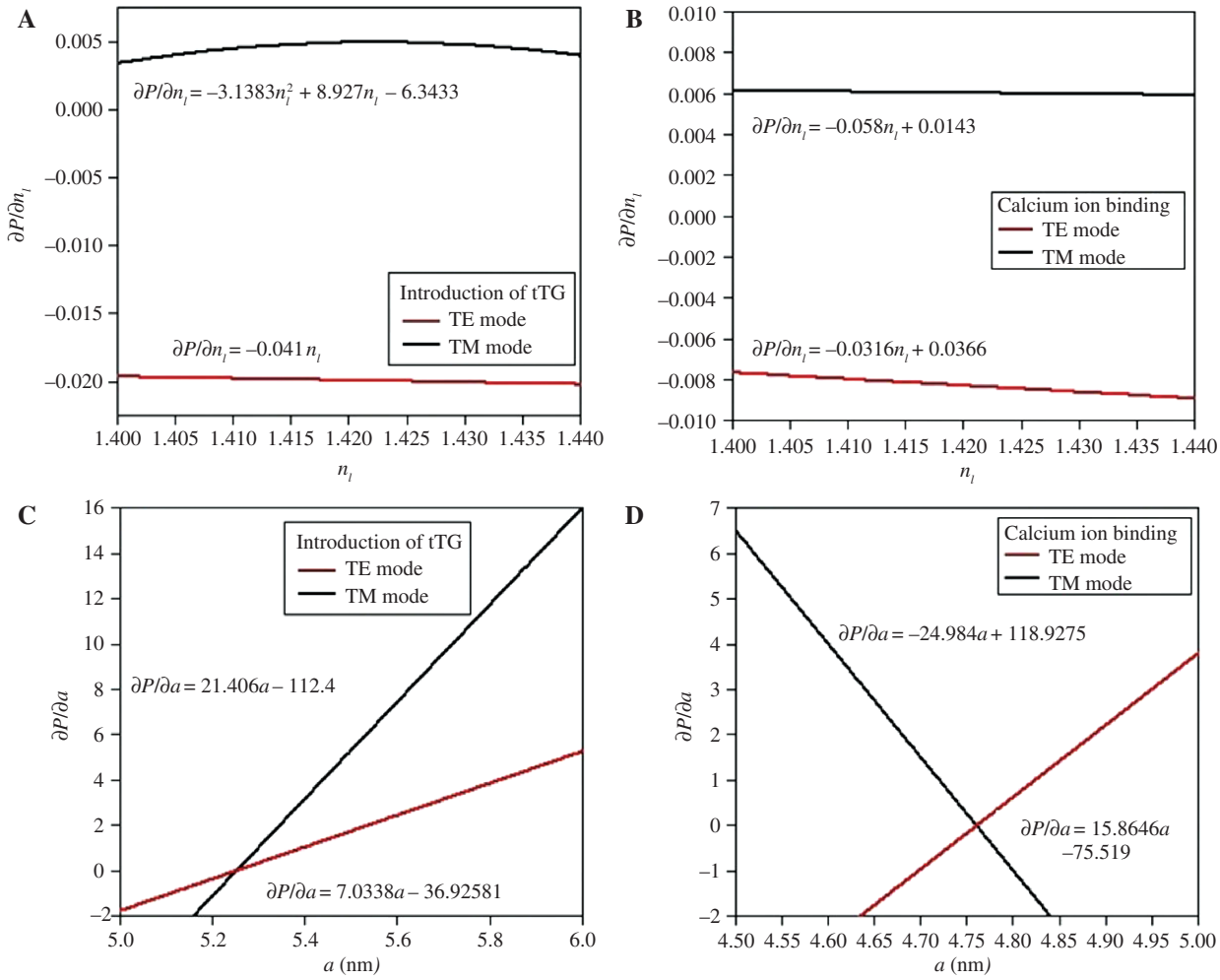

Figure 7: Partial derivative of the power versus adlayer index at $\lambda = 1.305$ μm for TE mode (A) and 1.303 μm for TM mode (B) and partial derivative of the power versus adlayer thickness at $\lambda = 1.305$ μm for TE mode (C) and 1.303 μm for TM mode (D).

where ΔP_i (i=TE, TM) is the normalized power variation at resonance dip (herein, $\lambda = 1.305$ μm. for TE mode and 1.303 μm for TM mode), $\partial P_i/\partial n_l$ (i=TE, TM) are the power changes caused by refractive index difference, and $\partial P_i/\partial a$ (i=TE, TM) are the power variations due to adlayer thickness changes. To investigate the effect of the biolayer refractive index on the intensity, we detect different values of intensity caused by the changes of n_l at various resonance wavelengths. Similarly, the influence of biolayer thickness on the intensity can be obtained. The terms $\partial P_i/\partial n_l$ and $\partial P_i/\partial a$ with fitting formulas are sketched in Figure 7. It is noteworthy that the terms Δn_l and Δa are the shifts in adlayer properties for each step compared to Tris buffer calibration. The calculated values by the mean of Eq. (1) share the similar results compared to experimental results [21]. The calculated adlayer index of protein tTG is 1.418 (1.4184 experimental data [21]) and the tTG layer thickness is 5.25 nm (5.261 nm experimental data [21]). After Ca^{2+} binding, the index and thickness of protein tTG are 1.426 and 4.76 nm, respectively, compared to experimental results (1.428 for biolayer index and 4.761 nm for biolayer thickness). Given the values of thickness and refractive index of biolayer, it is able to calculate the surface mass density through De Feijter's formula [22]: $G = a(n_l - n_s)/(dn/dc)$, where dn/dc is the refractive index increment, which in the case of protein is 0.186 $cm^3\ g^{-1}$. The densities of adlayer contributed by tTG protein and tTG-Ca^{2+} compound are 2.38 and 2.36 $cm^3\ g^{-1}$, respectively. Integrated with adlayer thickness and density, we can conclude that a thin dense layer formed as Ca^{2+} binds to tTG protein. This phenomenon can be explained as that tTG protein undergoes conformational change on binding to Ca^{2+}.

4 Conclusions

We have theoretically designed the integrated MZI biosensor and carried out a detailed investigation of modal

properties. The employment of the device for protein analysis has been largely discussed. We adopted power change detection at resonance dip to interpret the biological event taking place in the sensing arm. The intensity change detection can achieve much higher sensitivity in sensing small refractive index change of the ambient medium. An optic-electric detector can be employed, thus greatly cutting cost. Biolayer properties can be extracted via Eq. (1) in the text. Given the values of the thickness and refractive index of the biolayer, we can calculate the surface mass density during the binding event. Integrated with adlayer thickness and density, we can structurally characterize the protein layer. Therefore, the proposed device is a very potential technique to characterize protein conformation underlying biomolecular interactions. In addition, it lays a good basis for the follow-up work. The proposed device used in biochemical sensing experimentally has been planed to carry out.

Acknowledgments: The authors gratefully acknowledge the financial support for this work provided by the National Natural Science Foundation of China under grant nos. 61690221 and 61427816 (Funder id: 10.13039/501100001809). This work was also supported by the Collaborative Innovation Center of Suzhou Nano Science and Technology.

References

[1] Narayanaswamy R, Wolfbeis OS. *Optical Sensors*. Springer: Berlin, Heidelberg, 2004.
[2] Fan X, White IM, Shopova SI, Zhu H, Suter JD, Sun Y. Sensitive optical biosensors for unlabeled targets: a review. *Anal. Chim. Acta* 2008, 620, 8–26.
[3] Estevez MC, Alvarez M, Lechuga ML. Integrated optical devices for lab-on-a-chip biosensing applications. *Laser Photon. Rev.* 2012, 6, 463–487.
[4] Brosinger F, Freimuth H, Lacher M, Ehrfeld W, Geodig E, Katerkampc A, Spenerc F, Cammannc K. A label-free affinity sensor with compensation of unspecific protein interaction by a highly sensitive integrated optical Mach-Zehnder interferometer on silicon. *Sens. Actuators B* 1997, 44, 350–355.
[5] Kozma P, Kehl F, Ehrentreich-Förster E, Stamm C, Bier FF. Integrated planar optical waveguide interferometer biosensors: a comparative review. *Biosens. Bioelectron.* 2017, 58, 287–307.
[6] Homola J. Surface plasmon resonance sensors for detection of chemical and biological species. *Chem. Rev.* 2008, 108, 462–493.
[7] Hoa XD, Kirk AG, Tabrizian M. Towards integrated and sensitive surface plasmon resonance biosensors: a review of recent progress. *Biosens. Bioelectron.* 2007, 23, 151–160.
[8] Nenninger GG, Tobiska P, Homola J, Yee SS. Long-range surface plasmons for high-resolution surface plasmon resonance sensors. *Sens. Actuators B* 2001, 74, 145–151.
[9] Kovacs N, Patko D, Orgovan N, Kurunczi S, Ramsden JJ, Vondervizst F, Horvath R. Optical anisotropy of flagellin layers: *in situ* and label-free measurement of adsorbed protein orientation using OWLS. *Anal. Chem.* 2013, 85, 5382–5389.
[10] Swann MJ, Peel LL, Carrington S, Freeman NJ. Dual-polarization interferometry: an analytical technique to measure changes in protein structure in real time, to determine the stoichiometry of binding events, and to differentiate between specific and nonspecific interactions. *Anal. Biochem.* 2004, 329, 190–198.
[11] Fesus L, Davies PJ, Piacentini M. Apoptosis: molecular mechanisms in programmed cell death. *Eur. J. Cell Biol.* 1991, 56, 170–177.
[12] Zhang J, Song Q, Tian H, Zhang X, Wu H, Wang J, Yu C, Li G, Fan D, Yuan P. A double-ring Mach-Zehnder interferometer sensor with high sensitivity. *J. Phys. D Appl. Phys.* 2012, 45, 1–5.
[13] Salzberg CD, Villa JJ. Infrared refractive indexes of silicon germanium and modified selenium glass. *J. Opt. Soc. Am.* 1957, 47, 244–246.
[14] Lee HJ, Henry CH, Orlowsky KJ, Kazarinov RF, Kometani TY. Refractive-index dispersion of phosphosilicate glass, thermal oxide, and silicon nitride films on silicon. *Appl. Opt.* 1988, 27, 4104–4109.
[15] Johnson PB, Christy RW. Optical constants of transition metals: Ti, V, Cr, Mn, Fe, Co, Ni, and Pd. *Phys. Rev. B* 1974, 9, 5056–5070.
[16] Gao L, Lemarchand F, Lequime M. Exploitation of multiple incidences spectrometric measurements for thin film reverse engineering. *Opt. Express* 2012, 20, 15734–15751.
[17] Sun X, Dai D, Thylen L, Wosinski L. High-sensitivity liquid refractive-index sensor based on a Mach-Zehnder interferometer with a double-slot hybrid plasmonic waveguide. *Opt. Express* 2015, 23, 25688–25699.
[18] Dell'Olio F, Conteduca D, Cimineli C, Armenise MN. New ultrasensitive resonant photonic platform for label-free biosensing. *Opt. Express* 2015, 23, 28593–28604.
[19] Bartal G, Oulton RF, Sorger VJ, Zhang X. A hybrid plasmonic waveguide for subwavelength confinement and long range propagation. *Nat. Photonics* 2008, 2, 496–500.
[20] Akowuah EK, Gorman T, Haxha S. Design and optimization of a novel surface plasmon resonance biosensor based on Otto configuration. *Opt. Express* 2009, 17, 23511–23521.
[21] Karim K, Taylor JD, Cullen DC, Swann MJ, Freeman NJ. Measurement of conformational changes in the structure of transglutaminase on binding calcium ions using optical evanescent dual polarisation interferometry. *Anal. Chem.* 2007, 79, 3023–3031.
[22] De Feijter JA, Benjamins J, Veer FA. Ellipsometry as a tool to study the adsorption behavior of synthetic and biopolymers at the air-water interface. *Biopolymers* 1978, 17, 1759–1772.

Graphical abstract

Chen Chen, Xun Hou and Jinhai Si

Design of an integrated optics for transglutaminase conformational change

https://doi.org/10.1515/ntrev-2018-0022
Nanotechnol Rev 2018; x(x): xxx–xxx

Regular article: A novel integrated optics is performed in monitoring tTG and Ca^{2+} interaction and characterizing tTG conformation.

Keywords: dual polarizations; finite-element method; integrated optics; protein conformational change.